Supporting Information

Morphology-retained Photo-conversion Reaction of Anthracene Single Crystal: A New Approach for Organic Heterostructures

Minkyung Lee[‡,∥], *Chibeom Park*[‡,§], *Jungah Kim*[∥], *Jinho Lee*[∥], *Soyoung Kim*[∥], *Jin Young Koo*[*,§], *Hee Cheul Choi*[*,∥,§]

[∥]Department of Chemistry, Pohang University of Science and Technology (POSTECH), 77 Cheongam-ro, Namgu, Pohang 790-784, Korea

[§]Center for Artificial Low Dimensional Electronic Systems, Institute for Basic Science (IBS), 77 Cheongam-Ro, Pohang 790-784, Korea

Corresponding Author

* E-mail : choihc@postech.edu

* E-mail : comish@postech.ac.kr

Table of Contents

1: Experimental information

General experimental information: Chemical composition of photoreacted crystal was characterized by GC-MS (Bruker, 450-GC & 320-MS) and ^{1}H-NMR spectrometer (500 MHz, AVANCE). Especially, **AN** and **ANQ** molecules from **PC-ANQ12** (12-hr irradiation) crystal were detected by ^{1}H-NMR spectrometer (800 MHz, Bruker DRX 500 and 850 MHz) after they had been separated by plate thin layer chromatography (PTLC) technique, and referenced with the residual proton signals of CH_3CN-d_5. The PL images and signal were obtained using a fluorescence microscope (Olympus microscope) equipped with a fluorescence filter (λ_{ex} = 330 – 380 nm, λ_{em} = 420 nm long pass filter). The morphology of obtained crystals was characterized by scanning electron microscopy (SEM, JEOL, JSM-7410F). X-ray diffraction data was obtained from synchrotron X-ray source with 1.2398 Å. Note that the two theta values were rescaled to the conventional wavelength (Cu Kα= 1.54057 Å) for a better comparison with reference data.

Synthesis of anthracene (AN) platy crystal: The physical vapor transport process was performed by placing 10 mg of anthracene powder (Aldrich, Reagent Plus® 99%, melting point (T_m) = 210-215 °C) at the center of a tube-type furnace with a product-collecting Si substrate placed at the downstream end of the furnace. The vaporization temperature measured at the location of anthracene powder was 200 °C. The temperature at a Si substrate was 45 °C, and the growth run for 12 min after the furnace reached at 200 °C (flow rate of carrier Ar = 200 sccm) produced colorless platy crystals. The product was used without further purification. ^{1}H NMR (500 MHz, CH_3CN-d_5) δ 8.096 (q, 4H, J = 3.5 Hz), 7.538 (q, 4H, J = 3.5 Hz), 8.551 (s, 2H)

Synthesis of photo-converted anthraquinone (PC-ANQ) platy crystal: The photo-oxidation on **AN** platy crystal was performed under mercury lamp light in oxygen atmosphere. **PC-ANQ12** (12-hr irradiation) and **PC-ANQ36** (36-hr irradiation) crystals were obtained depending on photoreaction times. The product was used without further purification. ^{1}H NMR of **PC-ANQ36** (irradiated 36h) (500 MHz, CH_3CN-d_5) δ 8.31 (q, 4H, J = 3.5 Hz), 7.92 (q, 4H, J = 3.5 Hz) 1H NMR of **PC-ANQ12** (irradiated 12h) (500 MHz, CH_3CN-d_5) δ 8.31 (q, 4H, J = 3.5 Hz), 7.92 (q, 4H, J = 3.5 Hz), δ 8.096 (q, 4H, J = 3.5 Hz), 7.538 (q, 4H, J = 3.5 Hz), 8.551 (s, 2H).

Synthesis of photo-converted dipara-anthracene (PC-DPA) platy crystal: The photo-dimerization on **AN** platy crystal was performed under mercury lamp light in argon atmosphere. The product was used without further purification. ^{1}H NMR (500 MHz, CH_3CN-d_5) δ 6.99 (q, 8H, J = 3.5 Hz), 6.82 (q, 8H, J = 3.5 Hz), 4.655 (s, 4H)

Synthesis of ANQ wire: To support the PL difference of photoreacted crystal, control experiments to grow ANQ wire were performed. **ANQ** crystals were grown by the same method used to grows **AN** platy crystals. The growth run for 12 min after the furnace reached at 300 °C (flow rate of carrier Ar = 200 sccm) produced yellow color wire crystals from **ANQ** powder (Aldrich, 97%, melting point (T_m) = 284-286 ^{o}C). The product was used without further purification. ^{1}H NMR (500 MHz, acetonitrile-d_5) δ 8.31 (q, 4H, J = 3.5 Hz), 7.92 (q, 4H, J = 3.5 Hz)

Device fabrication and measurement: A plate shape **AN** crystal was first transferred manually onto a substrate, where source and drain electrodes (3 nm Cr / 20 nm Au) were pre-patterned by

a conventional photolithographic technique, and its I_{DS}-V_{DS} curve was measured before and after the photo-conversion reaction. The channel length is fixed to be 10 μm, and the channel widths and thicknesses were obtained by atomic force microscopy (AFM) and optical microscope image, which were used to calculate the electrical conductivity. All the current measurements were conducted at ambient condition and room temperature using a Keithley 4200-SCS semiconductor characterization analyzer (Keithley Instruments Inc., Cleveland, OH, USA), with a Remote PreAmp (4200-PA) at room temperature in ambient condition. Triaxial cables were connected to the probe station to minimize the background noise. Due to a crystal folding, we could not measure the electrical property of heterostructure across the interface. This measurement takes the top priority in our near future research plan using an advanced measurement setup.

Area-selective photo-conversion reaction: The patterned crystal was prepared using an optical microscope combined with a photomask and excitation filter (λ_{ex} = 330 – 380 nm). The Photomask (250 nm Cr on quartz substrate) was fabricated using an e-beam lithography technique and chrome etching process. **AN** crystal on Si substrate is placed in a custom-made chamber equipped with quartz viewport and gas flow line. Photoreaction time was set to about 4 hours because an incomplete block of light in the current equipment results in slow reaction even at undesired area when the reaction time is longer than 4 hr.

Depth profile of heterostructure PL spectra: Depth profile PL spectra were obtained from 3 regions of **AN**/**PC-ANQ** heterostructure crystal using WITEC Alpha 300R Raman spectroscope with 355 nm laser excitation and 100x objective (NA= 0.9). The laser light was first focused on

the surface of substrate (height = 0 nm), and PL spectrum is sequentially taken by increasing the focal height with an increament of 10 nm up to the crystal thickness (240 nm).

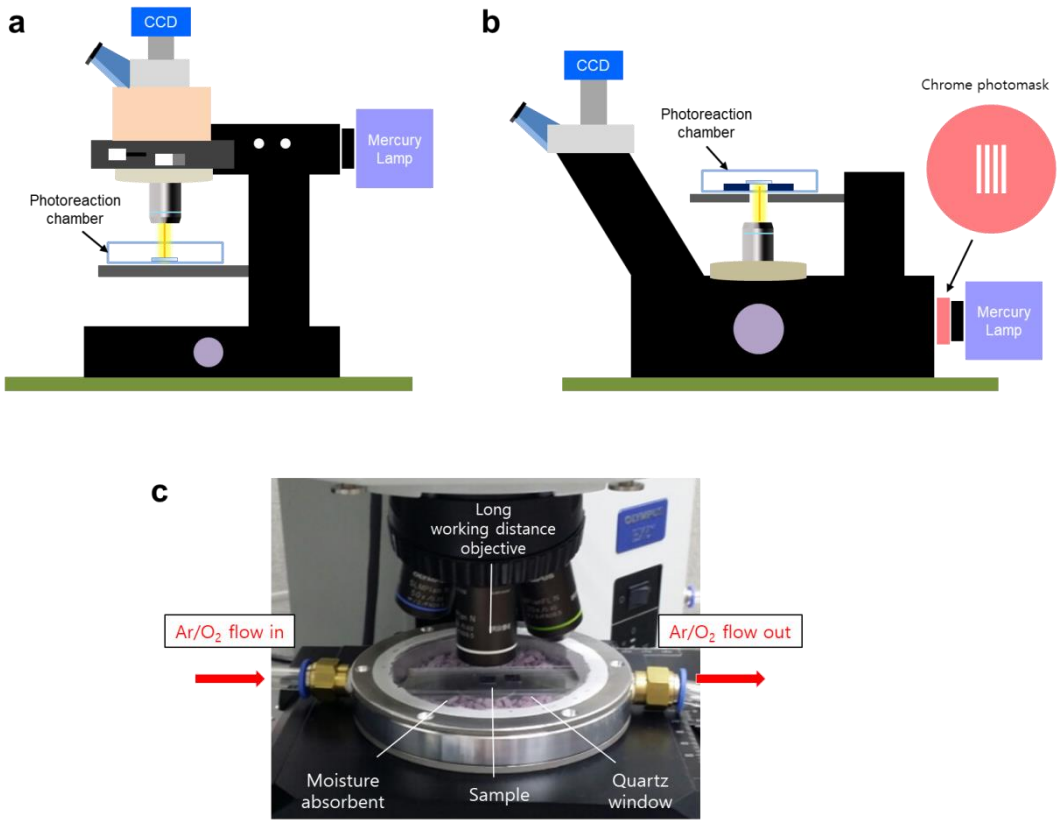

Scheme S1. Schematic photo-conversion reaction setup. a) Mercury lamp light irradiation on entire sample (flood exposure) b) Mercury lamp light irradiation through photomask (area-selective exposure) c) A photograph of photoreaction chamber equipped with Ar/O_2 flow line.

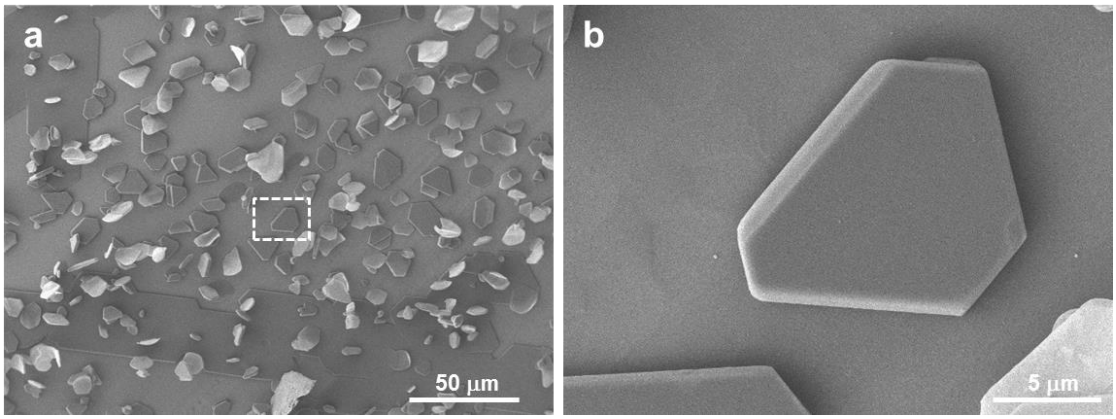

Figure S1. SEM images of anthracene platy crystal. a) Low- and b) high- magnification SEM image of as-grown **AN** platy crystals, respectively. The white dotted line in (a) is a mark for the high magnification SEM image in (b).

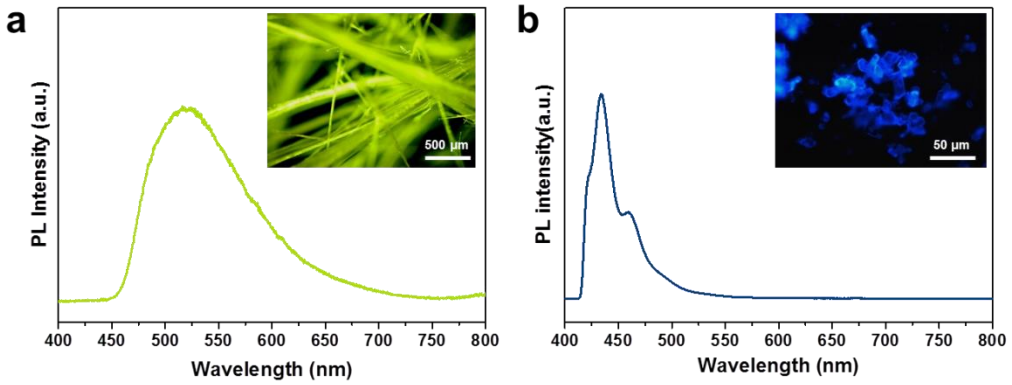

Figure S2. PL spectrum of a) **ANQ** wire grown by PVT process and b) As-purchased **DPA** powder. Insets are respective PL images.

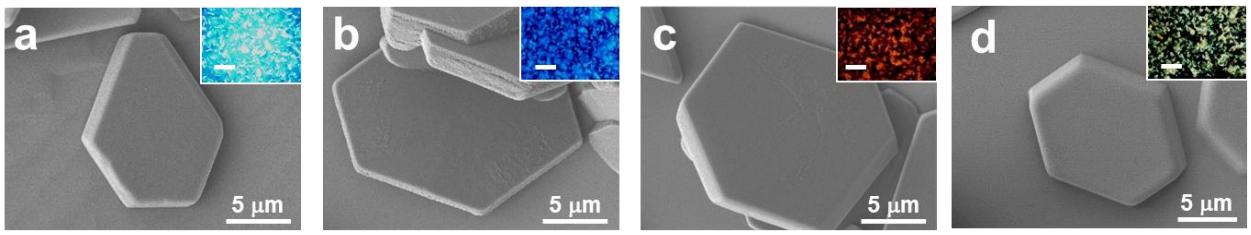

Figure S3. SEM images of a) as-grown **AN** platy crystals, b) **PC-DPA,** c) intermediate **PC-ANQ** (12hr reaction) and d) **PC-ANQ** (36hr reaction). All crystals were prepared from same batch of PVT-grown AN crystals. Inset images are photoluminescence images under mercury lamp light (λ_{ex} = 330 – 380 nm), and the scale bar is 5 μm.

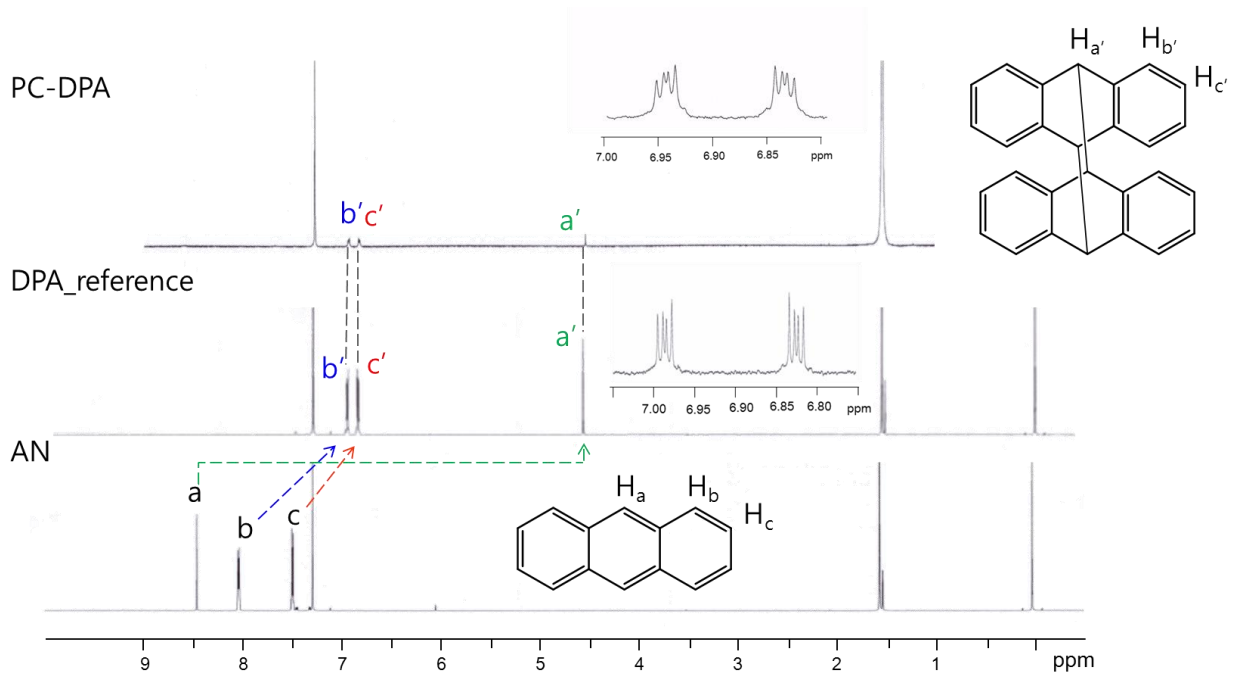

Figure S4. ^{1}H-NMR spectra of **PC-DPA** in $CDCl_3$. The aliphatic ($H_{a'}$) and aromatic protons ($H_{b'}$-$H_{c'}$) of **PC-DPA** shifted upfield, and the bridgehead C-H proton is shown at 4.57 ppm in **PC-DPA**

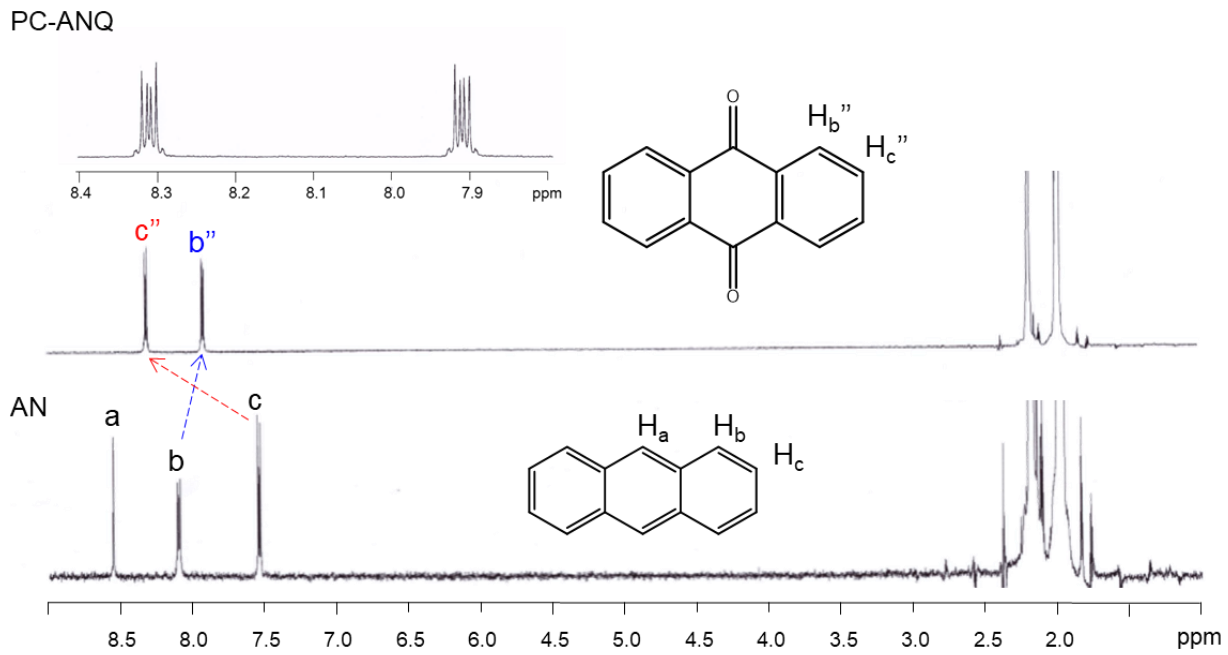

Figure S5. ^{1}H-NMR spectra of **PC-ANQ** in CD_3CN. The aromatic protons ($H_{c"}$) upon formation of **PC-ANQ** shifted downfield.

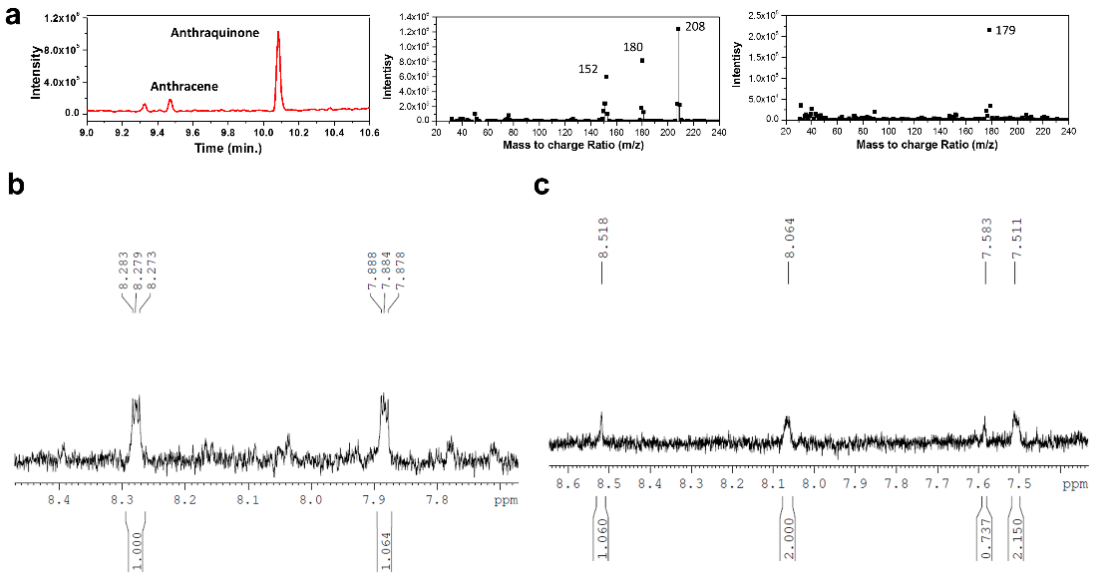

Figure S6. a) GC-MS and b, c) ^{1}H-NMR spectra of intermediate **PC-ANQ**. There are two components in **PC-ANQ** platy crystals, one is **AN** and the other is **ANQ**. **AN** was detected at 9.47 min (minor component) and **ANQ** was detected at 10.08 min (major component). The MS data show m/z of 208 and 179, which are corresponding to **ANQ** and **AN** molecular weight, respectively. Each component was separated by PTLC column and examined ^{1}H-NMR spectrum.

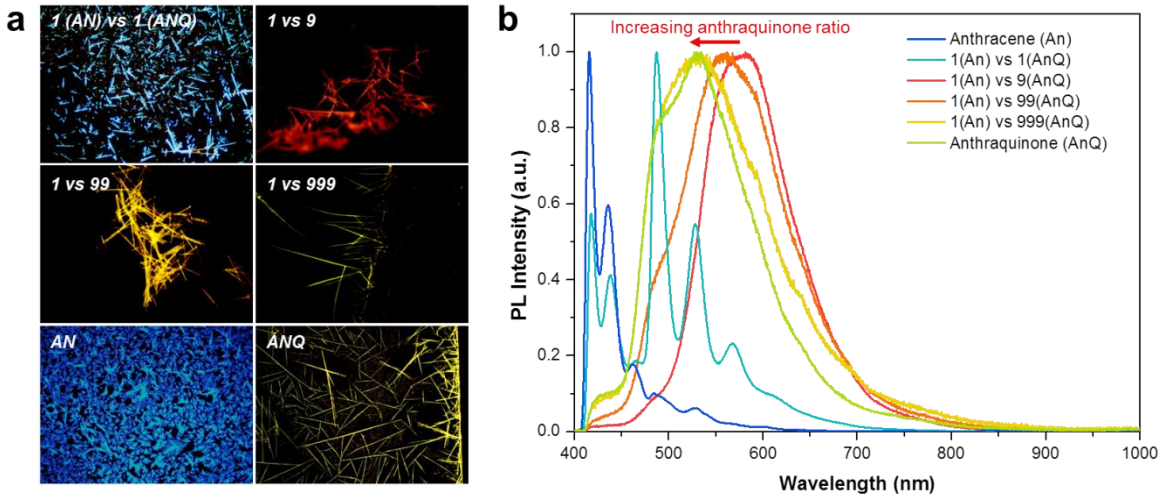

Figure S7. Photoluminescence (PL) of **AN/ANQ** mixture crystals depending on mixing ratio. a) PL images and b) PL spectra of **AN, ANQ**, and **AN/ANQ** mixture crystals prepared by liquid-liquid interfacial precipitation (LLIP) method. The maximum peak of PL is blue-shifted when **ANQ** ratio in the mixture is increased. Shifted PL tendency is similar to PL change of **PC-ANQ** (Figure 2b).

AN Sample	Resistance (Ω)	Length (μm)	Thickness (nm)	Width (μm)	Conductivity(S/cm)
1	2.45×10^{12}	10	257	378	4.20×10^{-10}
2	4.09×10^{13}	10	372	321	2.04×10^{-11}
3	1.90×10^{12}	10	211	141	1.76×10^{-9}
4	3.69×10^{12}	10	322	198	4.24×10^{-10}
5	3.86×10^{12}	10	155	151	1.11×10^{-9}
6	3.45×10^{12}	10	336	212	4.07×10^{-10}
7	3.81×10^{12}	10	54	186	2.63×10^{-9}
8	5.02×10^{13}	10	85	136	1.74×10^{-10}
9	3.60×10^{13}	10	237	161	7.27×10^{-11}
10	3.60×10^{13}	10	104	116	2.30×10^{-10}
11	4.95×10^{13}	10	226	97	9.18×10^{-11}
				Average	6.67×10^{-10}

Table S1. Electrical conductivity of tested **AN** crystals. The crystals showed average electrical conductivity of 6.67×10^{-10} S cm^{-1}.

PC-DPA Sample	Resistance (Ω)	Length (μm)	Thickness (nm)	Width (μm)	Irradiation time (hr)	Conductivity(S/cm)
1	1.18×10^{13}	10	322	198	5	1.33×10^{-10}
2	8.71×10^{12}	10	155	151	4	4.91×10^{-10}
3	9.17×10^{12}	10	321	207	5	1.63×10^{-10}
4	1.24×10^{13}	10	322	202	5	1.23×10^{-10}
					Average	2.28×10^{-10}

PC-ANQ Sample	Resistance (Ω)	Length (μm)	Thickness (nm)	Width (μm)	Irradiation time (hr)	Conductivity(S/cm)
1	1.68×10^{10}	10	315	95	2	1.99×10^{-7}
2	4.41×10^{10}	10	320	173	4	4.10×10^{-8}
3	1.68×10^{10}	10	145	130	2.5	3.16×10^{-7}
4	2.80×10^{10}	10	369	195	2.5	4.96×10^{-8}
5	7.10×10^{9}	10	257	378	4	1.45×10^{-7}
6	5.62×10^{10}	10	373	321	2	1.49×10^{-8}
7	1.00×10^{11}	10	212	141	0.5	3.35×10^{-7}
8	1.68×10^{10}	10	54	186	8	7.24×10^{-5}
9	4.41×10^{10}	10	84	136	8	6.03×10^{-6}
10	1.68×10^{10}	10	237	161	2	5.09×10^{-6}
11	2.80×10^{10}	10	104	116	10	2.78×10^{-5}
12	7.10×10^{9}	10	226	97	10	1.62×10^{-6}
					Average	9.50×10^{-6}

Table S2. Electrical conductivity of photo-converted crystals. The **PC-DPA** and **PC-ANQ** crystals showed average conductivity of 2.28×10^{-10} S cm^{-1} and 9.50×10^{-6} S cm^{-1}, respectively.

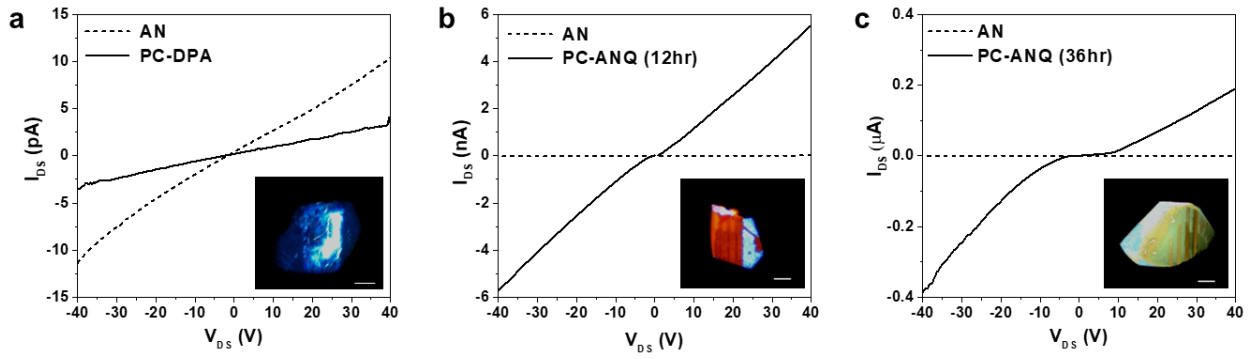

Figure S8. I_{DS}-V_{DS} curves of a) **PC-DPA**, b) **PC-ANQ** (12hr-irradiation) and c) **PC-ANQ** (36hr-irradiation) (solid line) with a comparison with I_{DS}-V_{DS} curves of starting **AN** crystal (dashed line). Respective PL images are shown as inset of each graph. (Scale bar: 40 μm) Note that the y-axis scale is different in each graph and the I-V profiles of starting **AN** crystals are all similar.

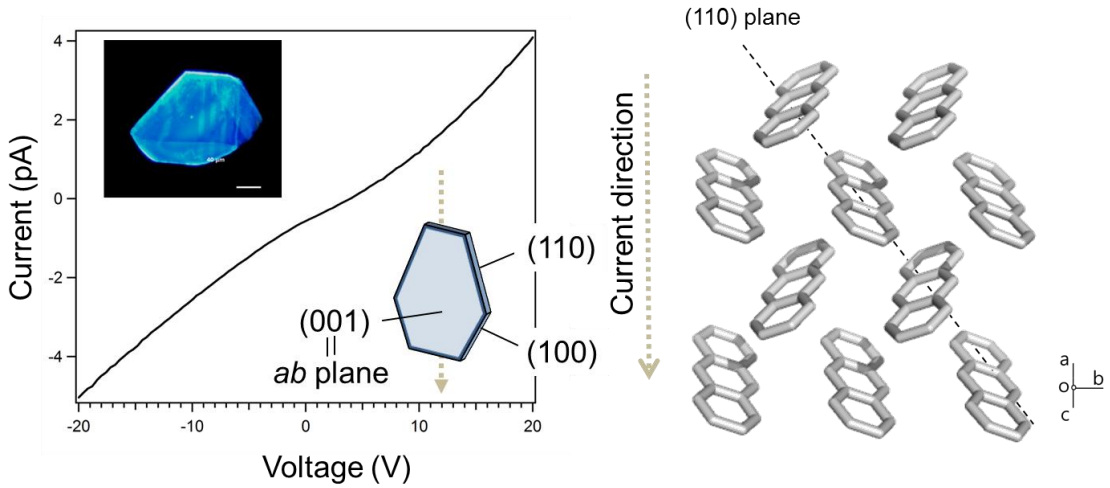

Figure S9. Face indexing of the **AN** single crystal. The crystallographic orientation was determined by face indexing of the **AN** single crystal on a Bruker APEX II QUAZAR instrument in-house. The Grey arrows indicate the direction of electrode connection, that is the direction of applied bias voltage, *i.e.*, enforced electrical current flow direction.

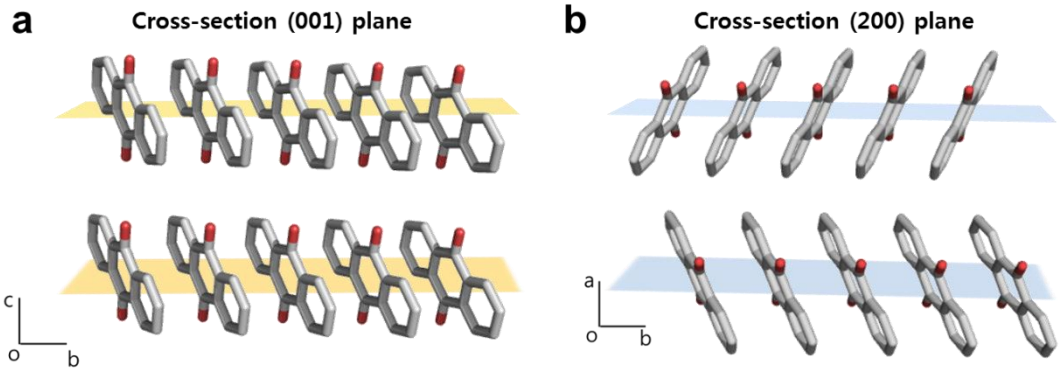

Figure S10. Schematic molecular arrangement in the cross-section of **PC-ANQ** a) (001) and b) (200) plane.

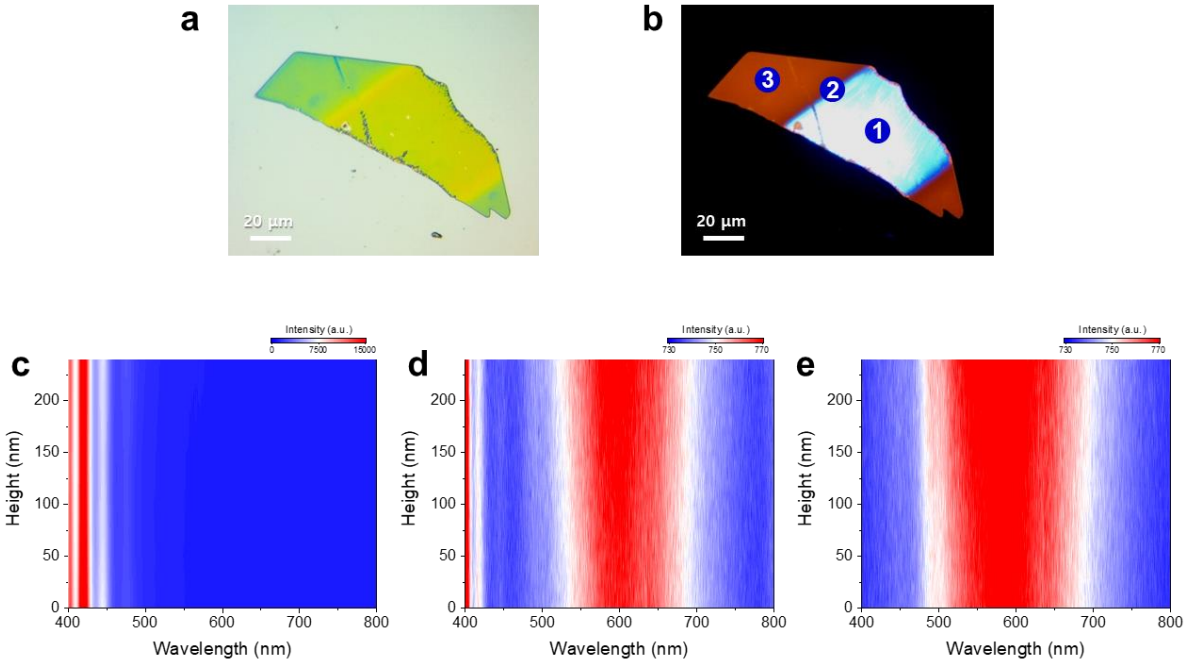

Figure S11. a) Optical microscope image and b) PL image of **PC-ANQ**/**AN**/**PC-ANQ** heterostructure. Depth profile of PL spectra obtained at c) **AN** region (marked by 1 in b)), d) **AN**/**PC-ANQ** boundary (marked by 2 in b)) and e) **PC-ANQ** region (marked by 3 in b)). The thickness of the crystal is 240 nm, as measured by AFM.

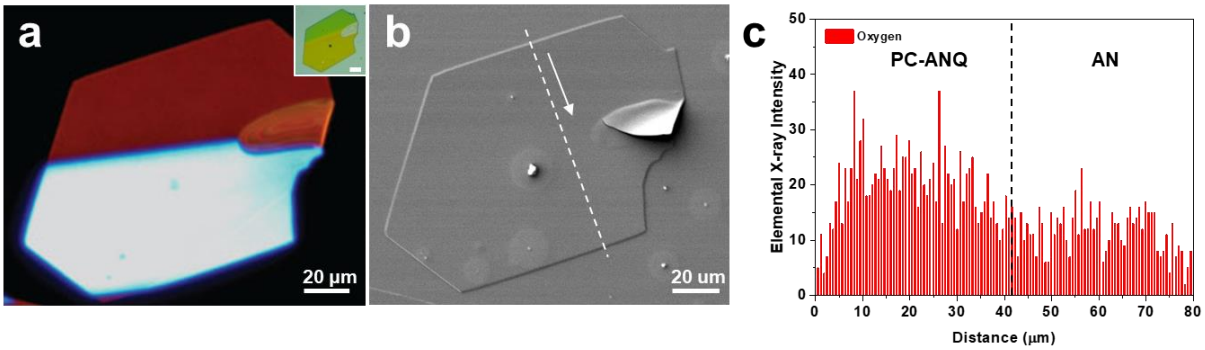

Figure S12. a) PL image, b) SEM image and c) EDS line profile across **AN/PC-ANQ** heterostructure, which indicates that the amount of oxygen molecules in **PC-ANQ** region is twice of that in **AN** region. Inset in a) is the optical image, where the scale bar is 10 μm.

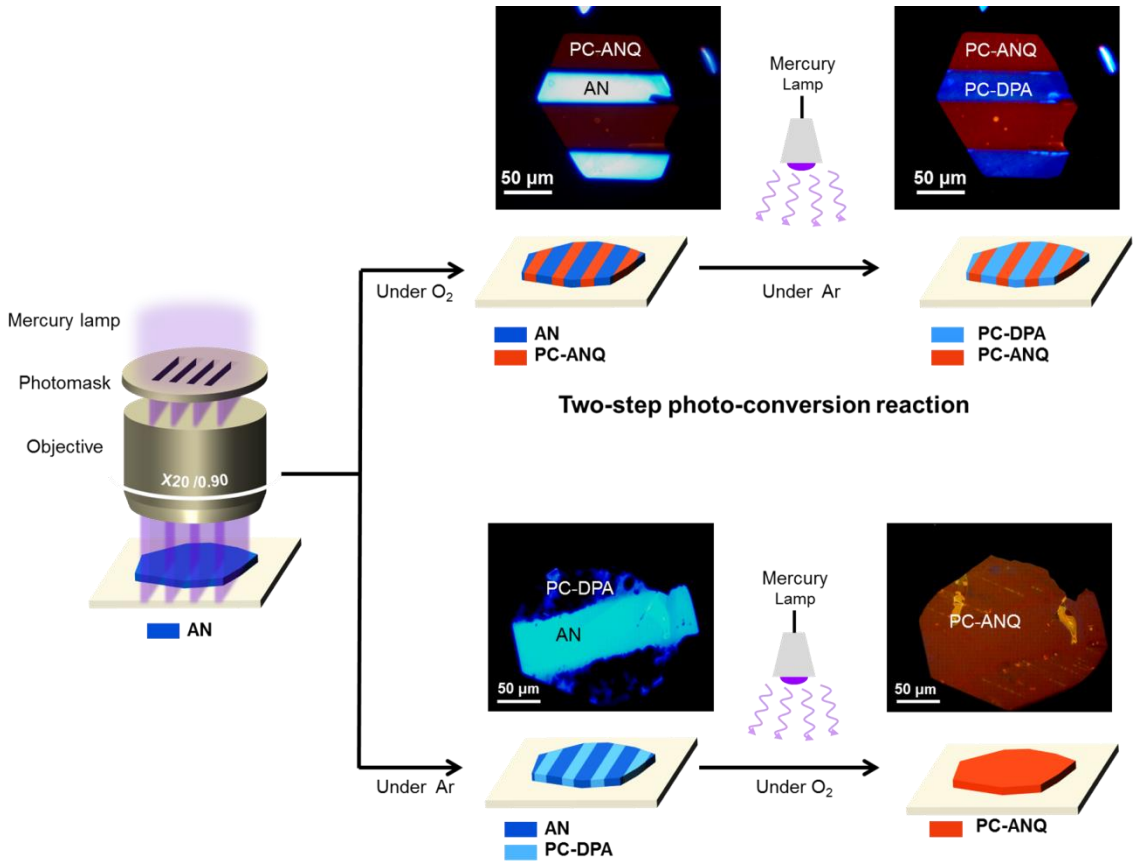

Figure S13. Area-selective photoreaction process. **PC-ANQ** is stable under mercury light irradiation in argon atmosphere, but **PC-DPA** is converted to **PC-ANQ** in the second photoreaction.

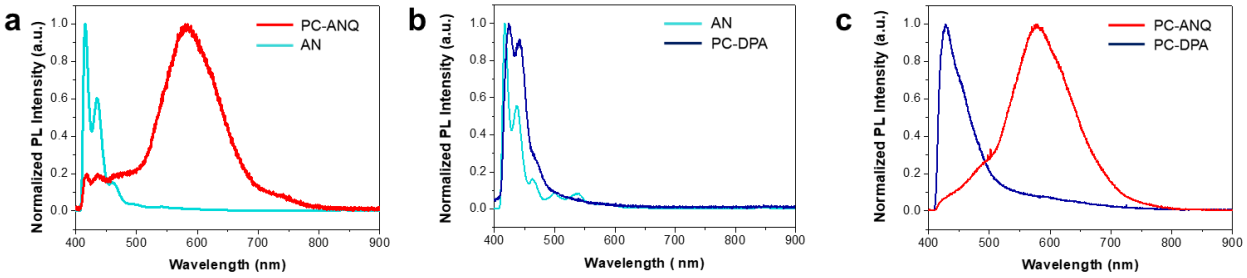

Figure S14. PL spectrum of each region in photo-converted heterostructure. a) **AN/PC-ANQ** b) **AN/PC-DPA** and c) **PC-ANQ/PC-DPA** heterostructure.